Research Article | Vol. 12, No. 11 / 1 Nov 2021 / Biomedical Optics Express 7024
Biomedical Optics EXPRESS

# Laser induced forward transfer isolating complex-shaped cell by beam shaping

PENG LIANG,[1,2] LINDONG SHANG,[1,2] YUNTONG WANG,[1,2] MARTIN J. BOOTH,[3] AND BEI LI[1,2,*]

[1]State Key Laboratory of Applied Optics, Changchun Institute of Optics, Fine Mechanics and Physics, Changchun, 130033, China
[2]University of Chinese Academy of Sciences, Beijing 100049, China
[3]Department of Engineering Science, University of Oxford, Parks Road, Oxford, OX1 3PJ, United Kingdom
*beili@ciomp.ac.cn

**Abstract:** Beam shaping techniques have been widely used in holographic optical tweezers to accurately manipulate tiny particles and hologram optimization algorithms have also been widely reported to improve the optical trapping performance. In this paper, we presented a beam shaping laser induced forward transfer (BS-LIFT) technique to isolate complex-shaped cells. To do this, we built up a BS-LIFT instrument which combined beam shaping methods and laser induced forward transfer using liquid-crystal-on-silicon spatial light modulator. The laser beam was modulated into multiple desired points at the focal plane employing the Gerchberg–Saxton (GS) algorithm. Feasibility was verified through transferring various samples. To our knowledge, this is the first demonstration of BS-LIFT applied to the transfer complex-shaped cells. We successfully transferred cells whose size ranged from 1 μm to 100 μm. Our design will provide a novel approach for the application of this beam shaping technique and the isolation of single cells with variable shapes.



## 1. Introduction

Single cell research is becoming an ever more important approach in the life sciences and the deterministic isolation of single cells is a critical step in such an approach [1]. However, the size of cells ranges from nanometers to micrometers and there can be large variability in their shapes. There are considerable challenges in isolating one single cell or bacterium from its environment based on existing isolation methods, such as Fluorescence-Activated Cell Sorting (FACS) [1,2], Magnet-Activated Cell Sorting (MACS) [3,4] and Laser Microdissection (LMD) [5], especially when the cell shape is complex. A widely applicable cell sorting method would be of great significance to single cell research.

Laser induced forward transfer (LIFT) has been employed to isolate single cells including bacteria in recent years [6,7]. Based on the principle of laser-material interaction, the biofilm absorbs the laser and produces an expansion force to push the cells that are adhered to the biofilm. For simple cells, like a spherical shaped cell, a single beam can accomplish the LIFT process. For cells with complex shapes, we combined image recognition and beam shaping algorithms to generate the light field corresponding to the target cell shape. Under the expansion force, the target cell is pushed into a receiver for subsequent research. We report the first demonstration of laser induced forward transfer of a single cell using a spatial light modulator, which could isolate complex-shaped single cell or bacteria by modulating the beam shape, shown in Fig. 1.

Adaptive optics, which employs adaptive elements to control the light field, has become a valuable tool in scientific research and industrial applications. These adaptive elements include liquid crystal spatial light modulators (SLMs), digital mirror devices (DMDs) and deformable mirrors (DMs). They can modulate the properties of a beam across its profile through modification of the phase, amplitude or polarization of the beam [8]. In laser material processing,

#439054 https://doi.org/10.1364/BOE.439054
Journal © 2021 Received 28 Jul 2021; revised 30 Sep 2021; accepted 4 Oct 2021; published 19 Oct 2021

Biomedical Optics EXPRESS

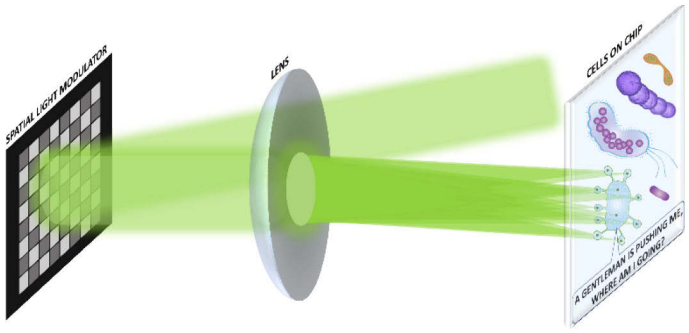


**Fig. 1.** Beam shaping laser induced forward transfer isolating complex-shaped bacteria cells.

adaptive elements were employed to correct the aberrations when focusing inside the workpiece [9], modulate the intensity distribution of focal plane to improve processing accuracy [10,11], fabricate particular shaped objects [12,13] or perform parallel processing [14]. In the field of optical microscopy, adaptive elements can mostly be used in two ways: in the illumination path and/or in the imaging path [15]. In the first case the illumination beam was shaped by adaptive elements for different applications, such as correcting aberrations in the scanning spot in confocal laser scanning microscopes [16], replacing the mechanical scanning by shifting the focal position in fluorescent probe scanning [17], or allowing 3D super-resolution imaging in stimulated emission depletion (STED) microscopy by producing an aberration corrected diffraction-limited ring-shaped focus to suppress the fluorescence of out-of-focus molecules [18,19]. In the second case, by using adaptive elements as programmable Fourier filters, the Fourier components of the light from the sample could be manipulated to influence the image contrast, which gives one complete freedom to implement new contrast mechanisms such as spiral phase contrast (SPC) [20,21], quantitative imaging and interferometry [22]. Besides, adaptive optics has also been widely used in optical tweezers [23,24], controlling the light distribution to form desired trap patterns, which could be employed to manipulate bacterial, cells [25] or ultracold atom [26] for different applications.

## 2. Methodology

### 2.1. Experimental set-up

The BS-LIFT instrument is shown in Fig. 2. A 40 μJ, 2 ns duration, 532 nm single pulse laser was focused on the surface of the LIFT chip, which included a 25 nm-thickness aluminum film on the glass surface. A pure-phase reflective liquid-crystal-on-silicon spatial light modulator (LCOS-SLM) with a pixel pitch of 8 μm and a resolution of $1920 \times 1200$ pixels was employed in this system, so that the laser beam on the focal plane, within known physical constraints, could be shaped to arbitrary desired forms. Both the LIFT chip and receiver were mounted on a translation stage. When we observed the bacteria or cell on the LIFT chip, the receiver was moved outside of the light path. After we had determined the target cell, the receiver was moved to the right place to receive the ejected cell.

### 2.2. Gerchberg–Saxton (GS) algorithm

Commonly-used algorithms that perform hologram calculation to obtain the target distribution of focal field could be divided into direct and iterative algorithms [24]. Direct algorithms include random mask (RM) encoding algorithm [27], superposition of prisms and lens (S) algorithm [28], and random superposition (SR) algorithm [29]; while iterative algorithms include

Biomedical Optics EXPRESS

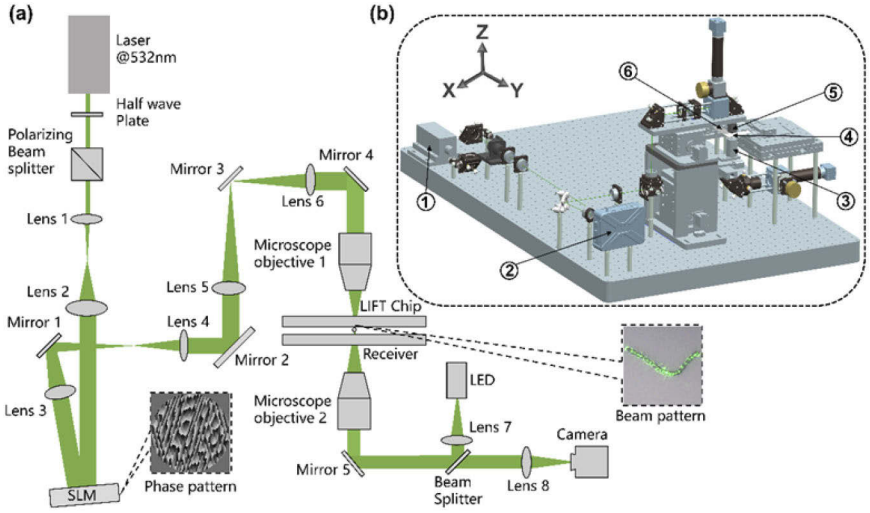


**Fig. 2.** (a) Light path diagram of the beam shaping laser induced forward transfer instrument. (b) The layout of the instrument, including ① the laser, ② the SLM unit, ③ the imaging microscope objective mounted on a Z-direction stage, ④ the ejecting chip mounted on a XY-direction stage, ⑤ the ejecting microscope objective controlled by another Z-direction stage, ⑥ the receiver mounted on another XY-direction stage. Laser: $\lambda = 532$ nm, 2 ns FWHM (full width half maximum), maximum pulsed energy of 40 μJ (Changchun New Industries Optoelectronics Technology Co., Ltd, China); SLM: maximal pattern rate of 60 Hz at 1920 × 1200 pixels with a pixel pitch of 8 μm, EXULUS-HD2 (Thorlabs, America); Imaging objective lens: 50×/NA0.6 TU Plan ELWD (Nikon, Japan); Ejecting objective lens: 10×/NA0.4 UPlanXApo (Nikon, Japan); Lens: all the lenses except Lens 8 are mounted achromatic doublet lens, 400–700 nm, Lens 1: f=15 mm, Lens 2: f=150 mm, Lens 3–6, f = 150 mm Lens 7: f=125 mm, Lens 8, ACL25416U-A (Thorlabs, America); Mirrors: all the mirrors used were protected-sliver coating mirror, PF10-03-P01 (Thorlabs, America); Half-wave plate: WPHSM05-532 (Thorlabs, America); Polarizing beam splitter: PBS251 (Thorlabs, America); Beam splitter: BSW10R (Thorlabs, America); LED: MNWHD2 (Thorlabs, America); CMOS camera: U3P630-H (Shenzhen DO3THINK Technology Co., Ltd, China).

the Gerchberg–Saxton (GS) algorithm [30], the adaptive-additive Gerchberg–Saxton (GAA) algorithm [23] and the weighted Gerchberg–Saxton (GSW) algorithm [31]. In practice, all the iterative algorithms can modulate complex and higher-quality light fields, but have higher computational cost than direct algorithms [24]. The GS algorithm was chosen in this research to modulate the light field on the focal plane into the target distribution.

### 2.3. Determination of the target laser intensity

The images of bacteria or cell could be obtained by the bottom microscope objective and imaging system. To modulate the beam into the shape of target cell, it's important to generate a binary graph containing the target point that corresponds to the target cell. For the determination of the target, we used two kinds of methods: image recognition and user definition. The image recognition could be summarized in 4 steps as follow.

Step1: Image binarization. The algorithm changed the picture into a binary graph only containing "0" and "1" according to each pixel's grayscale value, the threshold value needs to be carefully determined to present the outline of the cell.

Biomedical Optics EXPRESS

Step2: Filtering. The binary graph typically contains noise after binarization. We performed median filtering to remove salt and pepper noise, and mean filtering to remove Gaussian noise.

Step3: Expansion and corrosion. To make the cell's boundaries in the picture clearer, we performed expansion and corrosion algorithms on the image.

Step4: For long-shaped or large-area cells, generating a same spot shape with the cell is feasible, but generating multiple spots corresponding to the cell profile is more efficient. For the latter, the algorithm marked the "position" of "1" which represented the cell in the picture, then averaged the width and divided the length of the cell into multiple points. The number of points was user-defined, as shown in Fig. 3. We used 20 points including the end points in the experiment of ejecting Anabeana. Determination of target point. For multiple tiny cells such as yeast shown in the results, Fig. 4, the picture after expansion and corrosion could be used as the beam shaping target.

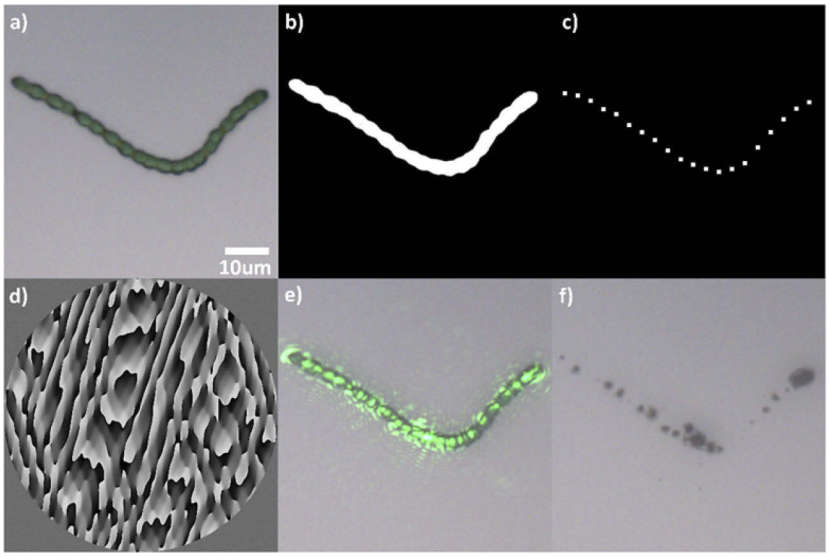


**Fig. 3.** Procedure of laser induced forward transfer (LIFT) combined with image recognition and beam shaping (see Visualization 1). a) Microscope imaging; b) Image binarization and filtering, the binary graph here "1" presents the outline of the cell; c) Determination of target point; d) Phase retrieval algorithm to calculate the phase graph corresponding to the target amplitude distribution; e) Modulate the laser beam into the target distribution; f) After ejection of the target cell.

The user definition method is designed for some complex-shaped cells or for images with non-uniform backgrounds, for which the image recognition could not perform very well. In the user definition mode, one could operate more freely by simply clicking the mouse at key points based on the microscope image, so that the algorithm could mark the points as the targets.

Biomedical Optics EXPRESS

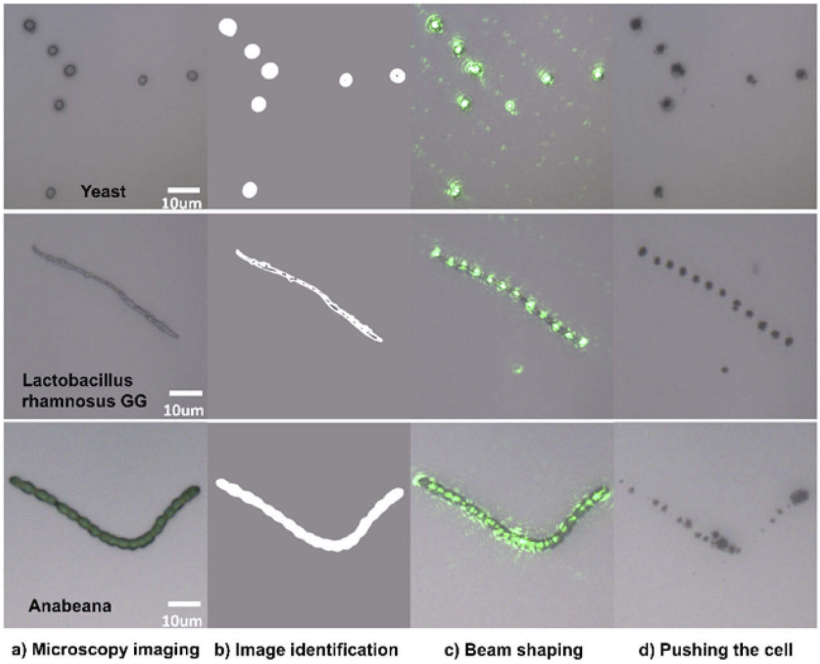


**Fig. 4.** Beam shaping laser induced forward transfer different size and shapes cell (seven single yeast cells, LGG and Anabeana cell) combined with image recognition algorithm. The bar represents 10 μm.

## 3. Results

### 3.1. Procedure of LIFT combined with beam shaping

The picture in Fig. 3. a was obtained by the bottom imaging system, and was then binarized to give the image in Fig. 3. b. Using the image in part b, the algorithm calculated the geometric center of the target and generated a target pattern that would produce several laser focal points (20 points in this case) in the focal plane. Then the picture was used as the target beam shape and a phase hologram was calculated by the Gerchberg–Saxton (GS) iterative algorithm to retrieve the phase distribution, as shown in Fig. 3. d. Then the phase pattern was loaded onto the LCOS-SLM which produced the target laser beam shape at the focal plane of the objective.

### 3.2. Image recognition and beam shaping for cells with different size and shape

Through beam shaping LIFT, we could modulate the light distribution of the focal plane into any patterns, within known physical constraints, according to the target such as yeast, Anabeana and LGG as shown in Fig. 4. The size of the target cells ranged from one micrometer to about one hundred micrometers. Furthermore, with a clean background, the image recognition algorithm performed well, as it could tell the yeast cell from E. coli by giving the size range that we know. The same method could also distinguish the E. coli cell from a more non-uniform background, as shown in Fig. 5.

### 3.3. User defined beam shaping for samples with complex background

For the sample with non-uniform background, which creates more difficulties for image recognition, we could determine the target light patterns distribution by selecting the key points through clicking the mouse (shown in Fig. 6). This user defined beam shaping method gives user more

Biomedical Optics EXPRESS

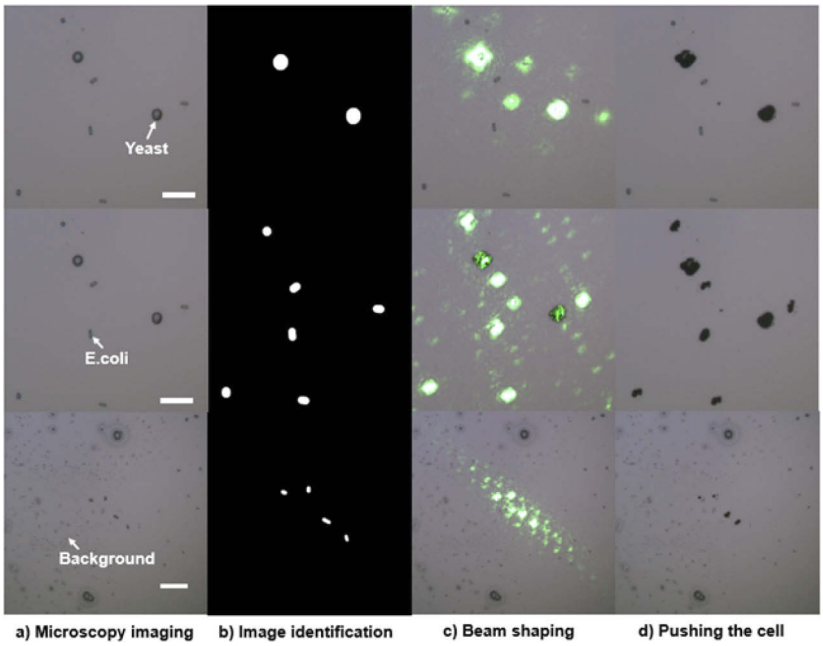


**Fig. 5.** Image recognition and beam shaping for different size cells and non-uniform background. The first line shows the algorithm can distinguish the yeast cell from the E. coli according to their size. The second line shows the algorithm can distinguish the E. coli cell from the yeast, the opposite process of the first line. The third line shows the algorithm can distinguish the E. coli cell from a non-uniform background. The bar represents 10 μm.

freedom for different kinds of cells in more complex samples. Glycerin was used to maintain the flagellate's viability, and the glycerin was also transferred with the flagellate, so the spots around the received flagellate (Fig. 6. f or Fig. 6. l) were the splashes of glycerin that landed on the receiver.

Biomedical Optics EXPRESS

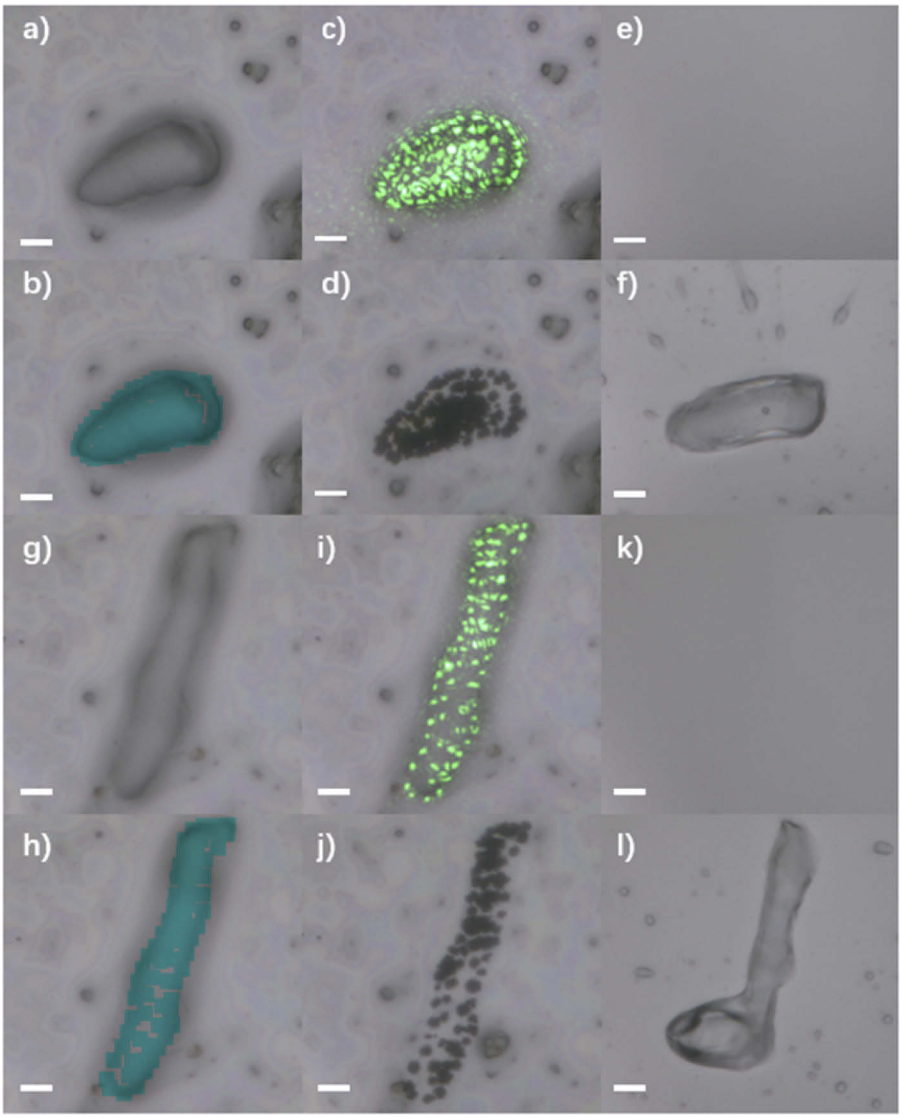


**Fig. 6.** Transfer and capture complex-shaped flagellate (see Visualization 2), the bar represents 10 μm. a): Image of flagellate before ejecting. b): The "ejecting position" defined by user's mouse clicks in the software. c): The laser was modulated by SLM and formed multiple focal points, which corresponded to the ejecting position. d): The flagellate was transferred, leaving some black holes visible on the chip. e): Nothing was visible on the receiver before transferring. f): The transferred flagellate was captured by the receiver. g): Image of flagellate before ejecting. h): The "ejecting position" defined by user's mouse clicking in the software. i): The laser was modulated by SLM and formed multiple focal points, which corresponded to the ejecting position. j): The flagellate was transferred and some black holes were visible on the chip. k): Nothing on the receiver before transferring. l): The transferred flagellate was captured by the receiver.

Biomedical Optics EXPRESS

## 4. Conclusion and outlook

We have demonstrated the procedure of LIFT combined with beam shaping and image recognition, and proved the feasibility of this technique for transfer complex-shaped cells such as long cells, which occupy a certain proportion of cells in nature and are difficult to be isolated by other method such as flow cytometry. Compared with other isolation methods, laser-based isolation is more precise and it can isolate the cell range from 1 μm to 100 μm in size. What's more, it is much easier to integrate into commonly-used commercial microscopes. However, there are still some aspects that can be improved. First, the GS type methods of beam shaping usually give speckle patterns within the illuminated area, which could be clearly seen in Fig. 6. Although our results have shown that we could avoid the impact of this on this work by increasing the ejecting points, a better algorithm that produces more uniform light field distribution could be beneficial for future study. Second, both the mechanical model of particles or cells in the liquid environment, and the relationship of laser parameters (energy and ejecting points) and the sample's shape and size, need to be systematically studied for a wide range of applications. Third, control software could be further developed to combine the different packages needed for development of automated cell identification and isolation.

**Acknowledgments.** The authors would like to thank Yan Yin and Hong Yang for providing the samples, and Chengmiao Sun for the help with the SLM software control.

**Disclosures.** The authors declare no conflicts of interest.

**Data availability.** Data underlying the results presented in this paper are available from the corresponding author upon request.

## References

1. P. Hu, W. Zhang, H. Xin, and G. Deng, "Single cell isolation and analysis," Front. Cell Dev. Biol. **4**, 1–12 (2016).
2. A. Gross, J. Schoendube, S. Zimmermann, M. Steeb, R. Zengerle, and P. Koltay, "Technologies for single-cell isolation," Int. J. Mol. Sci. **16**(8), 16897–16919 (2015).
3. A. Radbruch, "Small But Mighty : How the MACS 1 -Technology Based on Nanosized Superparamagnetic Particles has Helped to Analyze the Immune System Within the Last 20 Years," cytometry, 643–647 (2010).
4. B. Zhu and S. K. Murthy, "Stem cell separation technologies," Curr. Opin. Chem. Eng. **2**(1), 3–7 (2013).
5. K. DeCarlo, A. Emley, O. E. Dadzie, and M. Mahalingam, "Laser Capture Microdissection: Methods and Applications," in *Laser Capture Microdissection* Springer(2011), pp. 1–15.
6. N. T. Kattamis, P. E. Purnick, R. Weiss, and C. B. Arnold, "Thick film laser induced forward transfer for deposition of thermally and mechanically sensitive materials," Appl. Phys. Lett. **91**(17), 171120 (2007).
7. A. Marquez, M. Gómez-Fontela, and S. Lauzurica, "Fluorescence enhanced BA-LIFT for single cell detection and isolation," Biofabrication **12**(2), 025019 (2020).
8. P. S. Salter and M. J. Booth, "Adaptive optics in laser processing," Light: Sci. Appl. **8**(1), 110 (2019).
9. Y.-C. Chen, B. Griffiths, L. Weng, S. S. Nicley, S. N. Ishmael, Y. Lekhai, S. Johnson, C. J. Stephen, B. L. Green, G. W. Morley, M. E. Newton, M. J. Booth, P. S. Salter, and J. M. Smith, "Laser writing of individual nitrogen-vacancy defects in diamond with near-unity yield," Optica **6**(5), 662–667 (2019).
10. A. Mathis, F. Courvoisier, L. Froehly, L. Furfaro, M. Jacquot, P. A. Lacourt, and J. M. Dudley, "Micromachining along a curve: Femtosecond laser micromachining of curved profiles in diamond and silicon using accelerating beams," Appl. Phys. Lett. **101**(7), 071110 (2012).
11. M. K. Bhuyan, F. Courvoisier, P. A. Lacourt, M. Jacquot, R. Salut, L. Furfaro, and J. M. Dudley, "High aspect ratio nanochannel machining using single shot femtosecond Bessel beams," Appl. Phys. Lett. **97**(8), 081102 (2010).
12. R. Pohl, M. Jansink, G. R. B. E. Römer, and A. J. Huis in 't Veld, "Solid-phase laser-induced forward transfer of variable shapes using a liquid-crystal spatial light modulator," Appl. Phys. A **120**(2), 427–434 (2015).
13. R. C. Y. Auyeung, H. Kim, N. A. Charipar, A. J. Birnbaum, S. A. Mathews, and A. Piqué, "Laser forward transfer based on a spatial light modulator," Appl. Phys. A **102**(1), 21–26 (2011).
14. S. Hasegawa, H. Ito, H. Toyoda, and Y. Hayasaki, "Massively parallel femtosecond laser processing," Opt. Express **24**(16), 18513–18524 (2016).
15. C. Maurer, A. Jesacher, S. Bernet, and M. Ritsch-Marte, "What spatial light modulators can do for optical microscopy," Laser Photonics Rev. **5**(1), 81–101 (2011).
16. M. J. Booth, "Adaptive optics in microscopy," Phil. Trans. R. Soc. A. **365**(1861), 2829–2843 (2007).
17. P. J. Smith, C. M. Taylor, A. J. Shaw, and E. M. McCabe, "Programmable array microscopy with a ferroelectric liquid-crystal spatial light modulator," Appl. Opt. **39**(16), 2664–2669 (2000).
18. A. Barbotin, S. Galiani, I. Urbancic, C. Eggeling, and M. J. Booth, "Adaptive optics allows STED-FCS measurements in the cytoplasm of living cells," Opt. Express **27**(16), 23378–23395 (2019).

Biomedical Optics EXPRESS


19. T. J. Gould, D. Burke, J. Bewersdorf, and M. J. Booth, "Adaptive optics enables 3D STED microscopy in aberrating specimens," Opt. Express **20**(19), 20998–21009 (2012).
20. S. Fürhapter, A. Jesacher, S. Bernet, and M. Ritsch-Marte, "Spiral phase contrast imaging in microscopy," Opt. Express **13**(3), 689–694 (2005).
21. S. Bernet, A. Jesacher, S. Fürhapter, C. Maurer, and M. Ritsch-Marte, "Quantitative imaging of complex samples by spiral phase contrast microscopy," Opt. Express **14**(9), 3792–3805 (2006).
22. A. Jesacher, S. Fürhapter, S. Bernet, and M. Ritsch-Marte, "Spiral interferogram analysis," J. Opt. Soc. Am. A **23**(6), 1400–1409 (2006).
23. H. Kim, M. Kim, W. Lee, and J. Ahn, "Gerchberg-Saxton algorithm for fast and efficient atom rearrangement in optical tweezer traps," Opt. Express **27**(3), 2184–2196 (2019).
24. M. R. He, Y. S. Liang, P. R. Bianco, Z. J. Wang, X. Yun, Y. N. Cai, K. Feng, and M. Lei, "Trapping performance of holographic optical tweezers generated with different hologram algorithms," AIP Adv. **11**(3), 035130 (2021).
25. G. R. Kirkham, E. Britchford, T. Upton, J. Ware, G. M. Gibson, Y. Devaud, M. Ehrbar, M. Padgett, S. Allen, L. D. Buttery, and K. Shakesheff, "Precision assembly of complex cellular microenvironments using holographic optical tweezers," Sci Rep **5**(1), 8577 (2015).
26. A. L. Gaunt and Z. Hadzibabic, "Robust digital holography for ultracold atom trapping," Sci Rep **2**(1), 721 (2012).
27. M. Montes-Usategui, E. Pleguezuelos, J. Andilla, and E. Martín-Badosa, "Fast generation of holographic optical tweezers by random mask encoding of Fourier components," Opt. Express **14**(6), 2101–2107 (2006).
28. M. Reicherter, T. Haist, E. U. Wagemann, and H. J. Tiziani, "Optical particle trapping with computer-generated holograms written on a liquid-crystal display," Opt. Lett. **24**(9), 608–610 (1999).
29. M. Polin, K. Ladavac, S.-H. Lee, Y. Roichman, and D. G. Grier, "Optimized holographic optical traps," Opt. Express **13**(15), 5831–5845 (2005).
30. W. O. S. R. W. Gerchberg, "A practical algorithm for the determination of phase from image and diffraction plane pictures," Optik **35**, 237–246 (1972).
31. R. D. Leonardo, "Computer generation of optimal holograms for optical trap arrays," Opt. Express **15**(4), 1913–1922 (2007).